

Fast Track Communication

Effects of plasmon energetics on light emission induced by scanning tunneling microscopy

K Miwa^{1,4}, M Sakaue¹, B Gumhalter² and H Kasai^{1,3}¹ Department of Applied Physics, Osaka University, Suita, Osaka 565-0871, Japan² Institute of Physics, 10000, Zagreb, Croatia³ Center for Atomic and Molecular Technologies, Osaka University, Suita, Osaka 565-0871, JapanE-mail: kasai@dyn.ap.eng.osaka-u.ac.jp

Received 23 January 2014, revised 23 March 2014

Accepted for publication 25 March 2014

Published 9 May 2014

Abstract

A theoretical model of plasmon and molecular luminescence induced by scanning tunneling microscopy using a molecule-covered tip on clean metal surfaces is developed. The effects of coupling between molecular exciton and interface plasmon on the luminescence spectra are investigated for variable energy of plasmon modes by means of the nonequilibrium Green's function method. It is found that spectral features arising from interference between the processes of energy absorption by the molecule and interface plasmons appear near the energy of the excitonic mode. For the energy of plasmon above (below) the energy of excitonic mode, an additional peak structure appears in the energy range slightly below (above) the energy of the excitonic mode. Prominent peak and dip structures observed in recent luminescence experiments are interpreted by the developed theory whereby its utility in the fields of plasmonics and nanophotonics is demonstrated.

Keywords: molecular luminescence, interface plasmon, scanning tunneling microscopy, molecular vibration, exciton–plasmon coupling, nonequilibrium Green's function method, interference

(Some figures may appear in colour only in the online journal)

Luminescence from systems containing coupled molecular excitons and plasmons has attracted much attention in the studies of interaction of light with nanomaterials. Intense electromagnetic fields generated by interface plasmons are exploited to enhance the luminescence intensity of target molecules [1–3]. Recent studies have also suggested that the dynamics of molecules including luminescence and energy absorption can affect the optical properties mediated by interface plasmons [4–6]. Interplay between the dynamics of molecular excitons and interface plasmons gives rise to peculiar phenomena that cannot be explained by taking into account only the individual

field properties. Understanding of their interplay on the microscopic level is a prerequisite to interpretation of complex optical properties of these systems, enables novel insight into the complicated aspects of light-matter interaction and helps in developing new technologies utilizing the control of energy conversion among plasmons, excitons, and photons.

The highly localized tunneling current of a scanning tunneling microscope (STM) can be used as an atomic-scale source to induce light emission (LE) from the system. In STM-LE from clean and molecule-covered metal substrate, interface plasmons localized near the tip-sample gap region play important roles. It is well established that light emission from clean metal surfaces is due to the radiative decay of interface plasmons [7–9].

⁴ Present address: Surface and Interface Science Laboratory RIKEN, Wako, Saitama 351-0198, Japan

When a molecule is located near the gap region, there are two radiative processes, i.e. luminescence from interface plasmons and that from the molecule. For molecules directly adsorbed on a metal substrate, the charge and energy transfer between them lead to quenching of molecular luminescence and hence plasmon-mediated emission is dominant [10]. Intrinsic molecular luminescence associated with intramolecular electronic and vibrational transitions can be observed when molecules are electrically decoupled from the metal substrate by dielectric films or molecular multilayers [11, 12]. An intense electromagnetic field generated by interface plasmons is used to promote and control the molecular luminescence [13–15]. Furthermore, molecules can be excited by the energy transfer from interface plasmons that are excited by the tunneling current [15, 16]. Therefore, the dynamics of molecules (e.g. molecular luminescence and excitations) induced by energy transfer between molecules and interface plasmons plays an important role in STM-LE from molecules on metal substrates.

Direct experimental evidence of plasmon-mediated excitations of molecules comes from STM-LE measurements using the tip of a molecule-covered shaft over a clean metal surface [6]. Although no electron tunneling to molecules takes place, the observed spectra, which can be considered as the luminescence spectra of interface plasmons, show peak and dip structures. The positions of several structures match the peaks in molecular luminescence and absorption spectra. Thus, the dynamics of molecules including luminescence and energy absorption affect the luminescence spectral profiles of interface plasmons. To understand this from a microscopic point of view it is necessary to investigate the interplay between the dynamics of molecular excitons and plasmons within the framework of quantum many-body theory.

We have investigated the effects of coupling between a molecular exciton and an interface plasmon (exciton–plasmon coupling) on the luminescence properties using the nonequilibrium Green's function method [17–20]. The results have revealed that the enhancement of plasmon excitation by the molecular electronic and vibrational modes, the energy absorption by the molecule, and reabsorption of energy by interface plasmons lead to peak-, dip- and dent-structures in the plasmon luminescence spectra. Additional peak structures arise owing to the interference between these energy absorption processes. Hence, in addition to the dynamics of molecules, the dynamics of interface plasmons plays an essential role in determining their luminescence spectral profiles. In a recent experiment [6], luminescence spectra were observed by tuning the energy of plasmon modes affected by the tip-sample geometry (e.g. the tip shape). Hence, to interpret the experimental results using the predictions of theoretical models it is essential to investigate the luminescence properties as functions of the energy of plasmon modes.

In this paper we investigate the effects of exciton–plasmon coupling on STM-LE for variable energy of the plasmon modes and compare the calculated luminescence intensities with the experimental data reported in [6]. A schematic illustration of the luminescence processes is presented in figure 1. We describe these processes within the model developed in our previous study [20] which we extend so as to include the

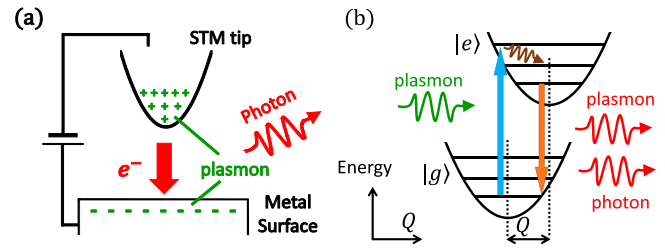


Figure 1. (a) Schematic picture of processes in which the tunneling current of STM drives the dynamics of the system by first exciting an interface plasmon, which then induces the creation of a molecular exciton through exciton–plasmon coupling and also emits a photon through coupling of plasmon to the photon field. (b) Schematic energy diagram of excitation and de-excitations in the adsorbed molecules whose excitation energy is close to the interface plasmon mode. Horizontal lines in each parabola denote vibrational sublevels where $|g\rangle$ and $|e\rangle$ denote the ground and first-excited electronic states, respectively. The variable Q denotes the vibrational coordinate whose equilibrium position is displaced by Q_0 upon the creation of a molecular exciton. The annihilation of the molecular exciton is induced by the emission of energy into interface plasmons or photons.

couplings of molecular exciton and interface plasmons to photons. The full model Hamiltonian of the system reads:

$$\mathcal{H} = H + H_{\text{ph}} + H_{\text{exc-ph}} + H_{\text{pl-ph}} \quad (1)$$

$$\begin{aligned} H = & \epsilon_{\text{ex}} d^\dagger d + \hbar\omega_0 b^\dagger b + \hbar\omega_p a^\dagger a \\ & + \sum_{\beta} \hbar\omega_{\beta} b_{\beta}^{\dagger} b_{\beta} + MQ_b d^\dagger d + V(ad^\dagger + da^\dagger) \\ & + \sum_{\beta} U_{\beta} Q_b Q_{\beta}, \end{aligned} \quad (2)$$

$$H_{\text{ph}} = \sum_l \hbar\nu_l \alpha_l^\dagger \alpha_l, \quad (3)$$

$$H_{\text{exc-ph}} = \sum_l (U_{\text{dl}} d^\dagger \alpha_l + U_{\text{dl}}^* d \alpha_l^\dagger), \quad (4)$$

$$H_{\text{pl-ph}} = \sum_l (U_{\text{al}} a^\dagger \alpha_l + U_{\text{al}}^* a \alpha_l^\dagger). \quad (5)$$

Here d^\dagger and d denote the creation and annihilation operators for the molecular excitonic mode with the energy ϵ_{ex} , respectively. For later convenience they are assumed to obey boson commutation rules. b^\dagger and b are creation and annihilation operators for the molecular vibrational mode with the energy $\hbar\omega_0$, respectively. Likewise, a^\dagger and a are for the interface plasmon mode with the energy $\hbar\omega_p$, b_{β}^{\dagger} and b_{β} are for the phonon mode β in a thermal bath, α_l^\dagger and α_l are for a photon mode l with the energy $\hbar\nu_l$, and $Q_b = b + b^\dagger$ and $Q_{\beta} = b_{\beta} + b_{\beta}^{\dagger}$. The parameters M , V , U_{β} , U_{dl} , and U_{al} describe the coupling between molecular exciton and a vibron (molecular-vibrational quantum), exciton–plasmon coupling, the coupling between the vibron and phonons in the thermal bath, the coupling between the molecular exciton and photons, and the coupling between interface plasmons and photons, respectively.

We next apply the Lang-Firsov (LF) canonical transformation $\tilde{\mathcal{H}} = e^S \mathcal{H} e^{-S}$ with $S = \lambda(b^\dagger - b) d^\dagger d$ and $\lambda = M/(\hbar\omega_0)$ to

remove the term $MQ_b d^\dagger d$ from $\tilde{\mathcal{H}}$ [20]. The LF transformed model Hamiltonian $\tilde{\mathcal{H}}$ is

$$\begin{aligned} \tilde{\mathcal{H}} = & \epsilon_{\text{ex}} d^\dagger d + \hbar\omega_0 b^\dagger b + \hbar\omega_p a^\dagger a + \sum_{\beta} \hbar\omega_{\beta} b_{\beta}^{\dagger} b_{\beta} \\ & + \sum_1 \hbar\nu_1 \alpha_1^{\dagger} \alpha_1 + V(ad^{\dagger} X^{\dagger} + da^{\dagger} X) + \sum_{\beta} U_{\beta} Q_b Q_{\beta}, \\ & + \sum_1 (U_{\text{dl}} d^{\dagger} X^{\dagger} \alpha_1 + U_{\text{dl}}^* d X \alpha_1^{\dagger}) + \sum_1 (U_{\text{al}} a^{\dagger} \alpha_1 + U_{\text{al}}^* a \alpha_1^{\dagger}), \end{aligned} \quad (6)$$

where $X = \exp[-\lambda(b^\dagger - b)]$. Here, the term including $d^\dagger d d^\dagger d$ is neglected. This approximation is expected to be valid, since the population of molecular excitons is low ($<10^{-4}$). The model Hamiltonian $\tilde{\mathcal{H}}$ can be utilized to investigate STM-LE from the molecular layers [15] as well as from clean metal surfaces using a molecule-covered tip [6] since the model parameter values included in H are expected to be of the same order in both cases [20].

The photon emission rate J_l of mode l is obtained from the average population of mode l :

$$J_l = \frac{d}{dt} \langle \alpha_l^{\dagger}(t) \alpha_l(t) \rangle_{\tilde{\mathcal{H}}}, \quad (7)$$

where $\langle \dots \rangle_{\tilde{\mathcal{H}}}$ denotes a statistical average in the representation in which the system evolution is governed by $\tilde{\mathcal{H}}$. The mode population is calculated from the photon correlation function $\langle \alpha_l^{\dagger}(t) \alpha_l(t) \rangle_{\tilde{\mathcal{H}}}$ which is related to the various Green's functions (quasiparticle propagators) on the Keldysh contour characterizing the dynamics of the system and generated by the Hamiltonian $\tilde{\mathcal{H}}$. In particular, this is the canonically transformed molecular excitonic propagator⁴:

$$L(\tau, \tau') = \frac{1}{i\hbar} \langle T_C \{ d(\tau) X(\tau) d^{\dagger}(\tau') X^{\dagger}(\tau') \} \rangle_{\tilde{\mathcal{H}}}, \quad (8)$$

and the plasmon propagator

$$P(\tau, \tau') = \frac{1}{i\hbar} \langle T_C \{ a(\tau) a^{\dagger}(\tau') \} \rangle_{\tilde{\mathcal{H}}}, \quad (9)$$

where τ is the Keldysh contour time variable and the operator T_C denotes the time ordering along the contour [22].

Assuming the steady-state, equation (7) can be expressed as (detailed derivation will be reported elsewhere):

$$J_l = |U_{\text{dl}}|^2 [-\mathfrak{L}^<(\nu_l)] + |U_{\text{al}}|^2 [-\mathfrak{P}^<(\nu_l)], \quad (10)$$

where $L^<$ and $P^<$ are the lesser projections of L and P , respectively [20]. The outgoing photon flux from the system is given by the sum over all photon modes l . Consequently, the luminescence spectra of the molecule and interface plasmons are obtained from the relations,

$$J_L(\omega) = - \sum_1 |U_{\text{dl}}|^2 \mathfrak{L}^<(\nu_1) \delta(\omega - \nu_1), \quad (11)$$

$$J_P(\omega) = - \sum_1 |U_{\text{al}}|^2 \mathfrak{P}^<(\nu_1) \delta(\omega - \nu_1). \quad (12)$$

⁴ For equivalent monopole electron and hole coupling to the vibron boson field the operators X and X^{\dagger} are absent from the polarization propagator, equation (8), see section 5C of [21].

The energy parameters U_{dl} and U_{al} satisfy the relations $U_{\text{dl}} \propto 1/\sqrt{\nu_1} \times d_{\text{mol}}$ and $U_{\text{al}} \propto 1/\sqrt{\nu_1} \times d_{\text{pl}}$, respectively [23]. Here, d_{mol} is the transition dipole moment of intramolecular electronic transition, on the order of a few Debye [16]. d_{pl} is the transition dipole moment of interface plasmons, on the order of several tens of thousand Debye [24]. In the case of STM-LE from a clean metal surface using a molecule-covered tip, U_{al} is considerably larger than U_{dl} . Then, the luminescence spectra detected experimentally are expected to correspond to J_P . For the molecules located between the metal substrate and the metal tip d_{mol} can be strongly enhanced [25] and thus J_L should be observable [11–15, 26, 27].

In STM-LE from molecular layers using a clean metal tip, the quenching of molecular luminescence caused by the energy transfer between molecules and metal substrates is suppressed, whereas it is relatively significant for a clean metal surface using a molecule-covered tip. Here, the energy transfer from electronically excited molecules is associated with electron-hole pair excitations in the metal substrate or the metal tip. When a molecule is directly adsorbed on the tip surface, a molecular exciton has a finite lifetime $1/\Gamma_{\text{ex}}$ due to the energy transfer to the metal tip (i.e. also for $V = 0$) and, therefore, the luminescence intensity of the molecule is suppressed [10]. For large Γ_{ex} the luminescence intensities of the molecule are expected to be much lower than that of interface plasmons. In this case the photon emission rate is approximately proportional to J_P . When the quenching is suppressed, J_L is expected to be detectable.

To investigate the excitation properties and analyze the structure of luminescence spectra, the spectral functions of the molecule ρ_L and of interface plasmons ρ_P are calculated using the relations $\rho_L(\omega) = -\mathfrak{L}^r(\omega)/\pi$ and $\rho_P(\omega) = -\mathfrak{P}^r(\omega)/\pi$. Here, L^r and P^r are the retarded projections of L and P , respectively. The Green's functions appearing in the above equations are calculated using the method described in [20]. In calculation of L , we have employed a random-phase-approximation (RPA)-type of diagrammatic series. Furthermore, the equation of motion (EOM) method is used to obtain the integral equations for the Green's functions of the molecular exciton, vibron and interface plasmons, where EOMs of these Green's functions are truncated at the second order in the exciton-plasmon coupling V . The obtained equations are self-consistently solved [20].

The parameters used in the calculations correspond to the STM-LE experiment with a tip covered by tetraphenylporphyrin (TPP) molecules and a silver surface for which $\epsilon_{\text{ex}} = 1.89$ eV and $\hbar\omega_0 = 0.16$ eV, respectively [6]. The values $\lambda^2 = 0.61$ and $2\pi\Sigma_{\beta} |U_{\beta}|^2 = 10^{-4}$ are taken from [20]. The presence of the tip induces an interface plasmon mode localized in the tip-sample gap region [28] and the energy of this mode is lower than $\hbar\omega_{\text{sp}} = 3.7$ eV typical of low index Ag surfaces [26, 29]. In view of this we take $\hbar\omega_p = 1.93, 2.00,$ and 2.17 eV which are consistent with experiments and earlier simulation results [26, 29].

A Markovian decay $\hbar\Gamma_{\text{pl}}$ is assumed for interface plasmons to give a plasmon lifetime of 4.7 fs for $V = 0$ [20]. One of the most dominant processes of nonradiative decay of an interface plasmon is electron-hole pair excitations in the metal substrate

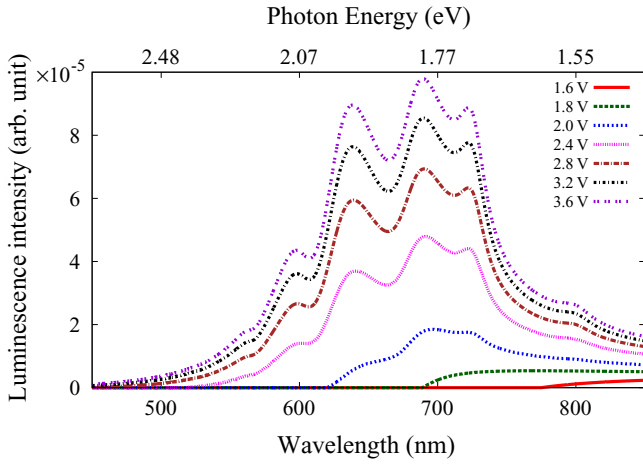


Figure 2. Bias voltage dependence of the luminescence spectra J_P of interface plasmons. Red solid, green dashed, blue dotted, magenta dotted, brown dashed-dotted, black dashed-dotted, and purple dotted lines are J_P 's at $V_{\text{bias}} = 1.6, 1.8, 2.0, 2.4, 2.8, 3.2,$ and 3.6 V. Exciton–plasmon coupling is $V = 0.08$ eV. The relaxation constant of a molecular exciton for $V = 0$ is $\Gamma_{\text{ex}} = 0.005$ eV. The energy of the plasmon mode is $\hbar\omega_p = 1.93$ eV.

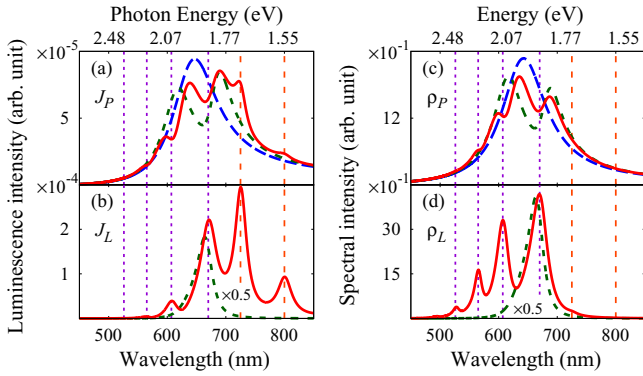


Figure 3. (a) Luminescence spectra of interface plasmons J_P , (b) luminescence spectra of the molecule J_L , (c) spectral function of interface plasmons ρ_P , and (d) spectral function of the molecule ρ_L . Red solid and blue dashed lines represent the results for $V = 0.08$ and 0.00 eV, respectively. Green dotted lines represent the results for $M = 0$ and $V = 0.08$ eV. The positions of peak structures in ρ_L are indicated by purple dotted lines. Orange dashed lines indicate the positions of peak structures at the wavelength $\lambda > 700$ nm in J_L . The relaxation constant of a molecular exciton for $V = 0$ is $\Gamma_{\text{ex}} = 0.005$ eV. The energy of the plasmon mode is $\hbar\omega_p = 1.93$ eV. The bias voltage is $V_{\text{bias}} = 3.2$ V.

or the metal tip [24]. Since the calculated luminescence spectra of interface plasmons for $V = 0$ has the peak width $\hbar\Gamma_{\text{pl}}$, this quantity is determined based on the luminescence spectral shape of interface plasmons reported in earlier experimental and simulation results [15, 16, 29].

Figure 2 shows J_P for various bias voltages V_{bias} . For $V_{\text{bias}} \leq 1.8$ V, J_P is a smooth curve, while for $V_{\text{bias}} \geq 2.0$ V, complicated peak and dip structures appear.

The positions of the peak structures near 725 and 800 nm in J_P (figure 3(a)) correspond to the peaks in J_L (figure 3(b)). The positions of the dip structures near 670, 607, 565, and 526 nm in J_P correspond to the peaks in ρ_L (figure 3(d)). The luminescence intensity of interface plasmons is suppressed in

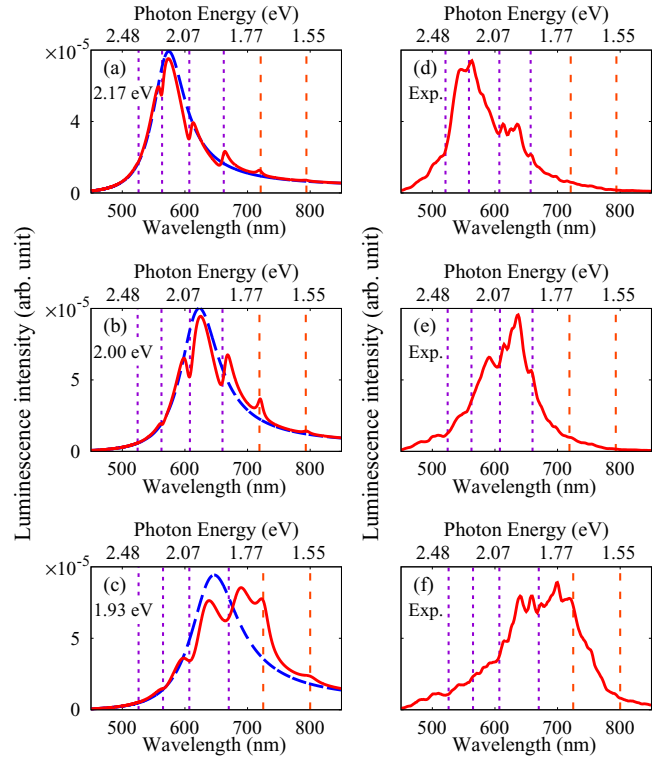


Figure 4. (a)–(c): Luminescence spectra of interface plasmons J_P for the energy of plasmon mode $\hbar\omega_p = 2.17$ eV, $\hbar\omega_p = 2.00$ eV, and $\hbar\omega_p = 1.93$ eV, respectively. Red solid and blue dashed lines represent the results for (a) $V = 0.05$ and 0.00 eV, (b) $V = 0.05$ and 0.00 eV, and (c) $V = 0.08$ and 0.00 eV, respectively. The positions of peak structures in spectral function ρ_L of the molecule are indicated by purple dotted lines. Orange dashed lines indicate the positions of peak structures at the wavelength $\lambda > 700$ nm in the luminescence spectra J_L of the molecule. The relaxation constant of the molecular exciton for $V = 0$ is (a) $\Gamma_{\text{ex}} = 0.005$ eV, (b) $\Gamma_{\text{ex}} = 0.010$ eV, and (c) $\Gamma_{\text{ex}} = 0.005$ eV, respectively. The bias voltage is $V_{\text{bias}} = 3.2$ V. (d)–(f): Measured luminescence spectra using molecule-covered tips with different tip shapes [6] shown for comparison.

the range of 600–675 nm, where the spectral intensity ρ_P is high (figure 3(c)). The additional peak structure appears in J_P around 690 nm.

We next analyze the origin of the above described structures. The peak structures are due to the enhancement of plasmon excitation by the molecular modes. The dip structures are due to the energy absorption by the molecule. The suppression of luminescence intensity is attributed to the reabsorption of energy by interface plasmons. The additional peak structure is attributed to interference between the energy absorption processes of the molecule and interface plasmons. These peak, dip, and additional peak structures are seen in the experimental spectra (see figure 4(f)). Thus, in STM-LE using a molecule-covered tip on a clean metal surface, the effects of interplay between the dynamics of the molecule and interface plasmons remarkably affect the luminescence spectra.

Figures 4(a) and (b) show J_P for $\hbar\omega_p = 2.17$ and 2.00 eV, respectively. For $\hbar\omega_p = 2.17$ eV, the peak structures enhanced by the molecular modes arise around 721 and 794 nm, while the dip structures due to energy absorption in the process of creation of molecular excitons arise near 662, 607, 563, and

526 nm. Asymmetric structures near 662 and 607 nm are due to the interference between the processes of energy absorption by the molecule and interface plasmons. For $\hbar\omega_p = 2.00$ eV, the peak and dip structures arise near 719 and 793 nm and near 660, 608, 563, and 524 nm, respectively. An asymmetric structure appears near 660 nm. These spectral features predicted by the present theory have indeed been detected in recent experiments (see figures 4(d) and (e)).

Inasmuch as the spectral profile of ρ_L , the energy of the plasmon mode plays an important role in the occurrence of dip structures in J_p . When $\hbar\omega_p$ matches the peak energy in ρ_L (e.g. for $\hbar\omega_p = 2.05$ eV), a dent structure caused by the reabsorption of energy by interface plasmons appears near $\hbar\omega_p$ in J_p [20]. The amplitude of the dip structures is large near $\hbar\omega_p$ because the product $P^{(0),r}L^r$, which controls the properties of the plasmon propagator (9), has a great effect on the spectral shape of J_p (see equation (50) in [20]). Here $P^{(0),r}$ is the retarded projection of the plasmon propagator for $V = 0$. The imaginary parts of $P^{(0),r}$ and L^r are related to the energy absorption processes of interface plasmons and the molecule, respectively. The product $\Im P^{(0),r}\Im L^r$ has a large value at the energies near the peak positions in ρ_L and $\rho_p^{(0)}$, where $\rho_p^{(0)} = -\Im P^{(0),r}/\pi$ exhibits a peak at $\hbar\omega_p$ (e.g. blue dashed line in figure 3(c)).

The effects of interference between the processes of energy absorption by the molecules and interface plasmons appear prominently near the energy E_{elastic} at which ρ_L reaches the maximum intensity. The product $\Re P^{(0),r}\Re L^r$ leads to the interference between the energy-absorption processes of the molecules and interface plasmons [20]. Since the real and imaginary parts of $P^{(0),r}$ satisfy Kramers–Kronig relations, $\Re P^{(0),r}$ is negative for $\hbar\omega < \hbar\omega_p$, and positive for $\hbar\omega > \hbar\omega_p$. Likewise, $\Re L^r$ is negative for $\hbar\omega < E_{\text{elastic}}$ and tends to be positive for $\hbar\omega > E_{\text{elastic}}$. Hence, $\Re P^{(0),r}\Re L^r$ gives a positive contribution to the plasmon luminescence intensity when $\hbar\omega$ is lower or higher than both E_{elastic} and $\hbar\omega_p$. On the other hand, $\Re P^{(0),r}\Re L^r$ tends to give a negative contribution when $\hbar\omega$ is between E_{elastic} and $\hbar\omega_p$ [20]. Since ρ_L exhibits a sharp peak near E_{elastic} , the absolute value of $\Re L^r$ is large near E_{elastic} . Thus, for $\hbar\omega_p > \epsilon_{\text{ex}}$, the additional peak structure appears in the energy range slightly below E_{elastic} . Also, the above described analysis indicates that for $\hbar\omega_p < \epsilon_{\text{ex}}$ the additional peak structures appear in the energy range slightly above E_{elastic} . We expect that this prediction can be verified experimentally, e.g. by analyzing the luminescence spectra in the case of lower-energy of plasmon modes, which is achieved by varying the tip-sample geometry [9, 15, 29, 30].

In conclusion, we have developed a microscopic model for interpretation of the luminescence spectral shapes of interface plasmons detected in scanning tunneling microscopy of clean metal surfaces using a molecule-covered tip. The spectra are strongly modified by the interference effects that give rise to additional peak structures around the energy of molecular excitonic mode. The calculated features of the peak, dip, and additional peak structures in the luminescence spectral shapes have been verified by comparison with the recent experimental findings [6]. Thereby the present results provide novel insight into the microscopic energy flow among interface plasmons,

molecular excitons and vibrons in the processes of light emission induced by the tunneling current. At a general level, the developed theoretical model elucidates dynamical properties of the systems in which multiply excited bosonic fields couple to each other and exchange energy. An understanding of the microscopic mechanisms underlying such complicated processes aids in revealing the fundamental nature of energy transfer between metal nanostructures and molecules, in the development of new techniques for microscopic control of energy flow, and in the design of new functional materials and photoelectric devices.

Acknowledgments

This work was supported in part by: MEXT Grants-in-Aid for Scientific Research on Innovative Areas Program (2203-22104008), Scientific Research Programs (A) (24246013), and Grants for Excellent Graduate Schools (130820-140331) ‘Atomically Controlled Fabrication Technology’; JST ALCA Program ‘Development of Novel Metal-Air Secondary Battery Based on Fast Oxide Ion Conductor Nano Thickness Film’ and Strategic Japanese-Croatian Cooperative Program on Materials Science ‘Theoretical Modeling and Simulations of the Structural, Electronic, and Dynamical Properties of Surfaces and Nanostructures in Materials Science Research’. Some of the numerical calculations presented here were performed using the computer facilities of the following institutes: CMC (Osaka University), ISSP, KEK, NIFS, and YITP. Special thanks are due to Professor R Berndt and Dr N L Schneider for providing the experimental data. The authors are deeply grateful to Prof W A Diño and Prof H Nakanishi of Osaka University for useful discussions.

References

- [1] Moskovits M 1985 *Rev. Mod. Phys.* **57** 783
- [2] Nie S and Emory S R 1997 *Science* **275** 1102
- [3] Lakowicz J R 2001 *Anal. Biochem.* **298** 1
- [4] Ishihara H, Nobuhiro A, Nakatani M and Mizumoto Y 2011 *J. Photochem. Photobiol. A: Chem.* **221** 148
- [5] White A J, Fainberg B D and Galperin M 2012 *J. Phys. Chem. Lett.* **3** 2738
- [6] Schneider N L and Berndt R 2012 *Phys. Rev. B* **86** 035445
- [7] Berndt R, Gimzewski J K and Johansson P 1991 *Phys. Rev. Lett.* **67** 3796
- [8] Uehara Y, Fujita T and Ushioda S 1999 *Phys. Rev. Lett.* **83** 2445
- [9] Rossel F, Pivetta M and Schneider W D 2010 *Surf. Sci. Rep.* **65** 129
- [10] Hoffmann G, Libioulle L and Berndt R 2002 *Phys. Rev. B* **65** 212107
- [11] Qiu X H, Nazin G V and Ho W 2003 *Science* **299** 542
- [12] Dong Z C, Guo X L, Trifonov A S, Dorozhkin P S, Miki K, Kimura K, Yokoyama S and Mashiko S 2004 *Phys. Rev. Lett.* **92** 086801
- [13] Uemura T, Furumoto M, Nakano T, Akai-Kasaya M, Saito A, Aono M and Kuwahara Y 2007 *Chem. Phys. Lett.* **448** 232
- [14] Liu H W, Nishitani R, Han T Z, Ie Y, Aso Y and Iwasaki H 2009 *Phys. Rev. B* **79** 125415
- [15] Dong Z C *et al* 2010 *Nature Photon.* **4** 50
- [16] Tian G and Luo Y 2011 *Phys. Rev. B* **84** 205419

- [17] Kadanoff L P and Baym G 1962 *Quantum Stat. Mech.* (New York: Benjamin) p 203
- [18] Miwa K, Sakaue M and Kasai H 2013 *J. Phys. Soc. Japan* **82** 063715
- [19] Miwa K, Sakaue M and Kasai H 2013 *Nanoscale Res. Lett.* **8** 204
- [20] Miwa K, Sakaue M and Kasai H 2013 *J. Phys. Soc. Japan* **82** 124707
- [21] Gumhalter B 1984 *Prog. Surf. Sci.* **15** 1
- [22] Keldysh L V 1965 *Sov. Phys. JETP* **20** 1018
- [23] Zhang Y, Zelinskyy Y and May V 2013 *Phys. Rev. B* **88** 155426
- [24] Persson B N J and Baratoff A 1992 *Phys. Rev. Lett.* **68** 3224
- [25] Mills D L 2002 *Phys. Rev. B* **65** 125419
- [26] Ino D, Yamada T and Kawai M 2008 *J. Chem. Phys.* **129** 014701
- [27] Fujiki A, Miyake Y, Oshikane Y, Akai-Kasaya M, Saito A and Kuwahara Y 2011 *Nano. Res. Lett.* **6** 347
- [28] Johansson P, Monreal R and Apell P 1990 *Phys. Rev. B* **42** 9210
- [29] Aizpurua J, Apell S P and Berndt R 2000 *Phys. Rev. B* **62** 2065
- [30] Rendell R W, Scalapino D J and Mühlischlegel B 1978 *Phys. Rev. Lett.* **41** 1746